

# SWELLING DURING PYROLYSIS OF FIBRE–RESIN COMPOSITES WHEN HEATED ABOVE NORMAL OPERATING TEMPERATURES

BRENT C. HOUCHEMS<sup>1</sup>, SARAH N. SCOTT<sup>1</sup>, VICTOR E. BRUNINI<sup>1</sup>, ELIZABETH M. C. JONES<sup>2</sup>,  
MICHAEL M. MONTOYA<sup>2</sup>, WENDY FLORES-BRITO<sup>2</sup> & KATHRYN N. G. HOFFMEISTER<sup>2</sup>

<sup>1</sup>Sandia National Laboratories, California, USA

<sup>2</sup>Sandia National Laboratories, New Mexico, USA

## ABSTRACT

It is experimentally observed that multilayer fibre–resin composites can soften and swell significantly when heated above their designed operating temperatures. This swelling is expected to further accelerate the pyrolysis, releasing volatile components which can ignite in an oxygenated environment if exposed to a spark, flame or sufficiently elevated temperature. Here the intumescent behaviour of resin-infused carbon-fibre is investigated. Preliminary experiments and simulations are compared for a carbon-fibre sample radiatively heated on the top side and insulated on the bottom. Simulations consider coupled thermal and porous media flow.

*Keywords:* pyrolysis, carbon-fibre, porous media flow.

## 1 INTRODUCTION

In an accident leading to a fire, heated fibre–resin composites can be an additional fuel source. For example, modern passenger aircraft can have airframes with well above 50% composite construction, by volume and weight [1]. This added fuel source could significantly exacerbate any aircraft fire scenario, such as the recent auxiliary power unit battery fire [2]. Even without direct exposure to flame, composites heated above their designed operating ranges can first begin to soften and swell as they move through their glass transition temperature. Further heating leads to the onset of pyrolysis where liquid and gaseous products can be produced, leading to further expansion. These gases can be ignited by a spark or other sufficiently hot heat source. For carbon-fibre, the fibre itself is an additional source of fuel for combustion [3].

Here multilayer carbon-fibre composites were heated to above their designed operating temperatures but below ignition temperatures leading to pyrolysis. Swelling of the samples was measured through both visible light edge detection and digital image correlation (DIC) on the top surface. Thermographic phosphors were selected for their ability to remotely monitor the temperature on the surface with minimal invasiveness [4]. Additionally, thermographic phosphors were included between several of the carbon-fibre layers before the samples were cured, following techniques developed in previous studies [5]. Pyrolyzed gases produced in the interior of the sample flow through the porous media matrix of carbon-fibre, resin and char to the boundaries of the sample. Some phosphors are transported along with these gases and escape from the top, bottom, and edge of the sample. Laser excitation of these phosphors provides an indication of the flow of these pyrolyzed gases from the interior of the sample through the porous media.

Thermocouples were used to measure both the heater temperature and the backside temperature of the sample. An infrared (IR) camera was focused on the top of the sample to determine surface temperatures during the heating. Additionally, video and still images of the burn were recorded throughout. The goal of this paper is to experimentally measure the



thickness change of the composite and demonstrate a model into which this thickness change can be incorporated.

## 2 HEATING CONFIGURATION

Experiments and computations were performed on disks of 6-layer carbon-fibre composites consisting of 33.8% prepreg epoxy by weight before curing. The samples were initially 12.7 cm in diameter and 2.5 mm thick. The geometric configuration of the sample under the heating element is shown in Fig. 1.

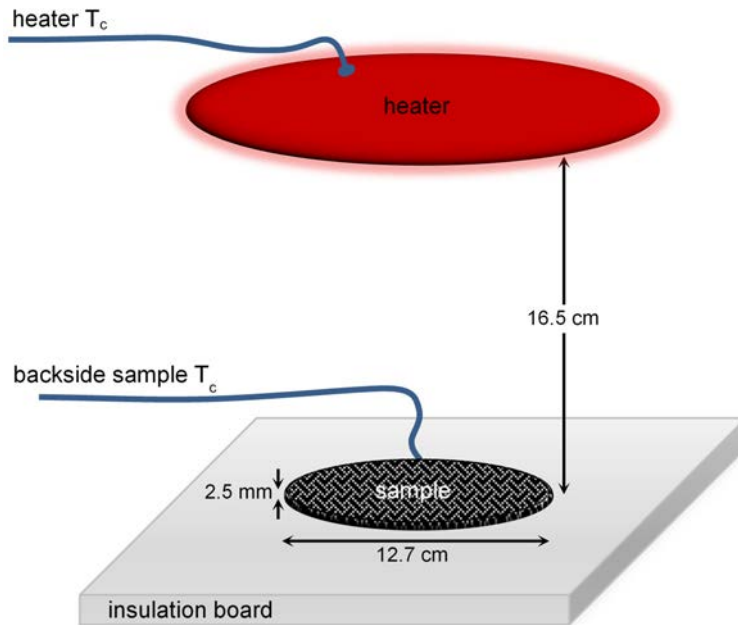


Figure 1: Carbon-fibre (6 layer) sample in the heating configuration with the backside sample thermocouple between the sample and insulation board.

The samples were heated directly on insulation board. The temperatures of both the heater and backside of the sample were measured with thermocouples. The incident heat flux was characterized by repeating the experiment with the sample replaced by an Inconel plate with known properties.

### 2.1 Decomposition mechanism

Previous experimental studies using thermogravimetric analysis (TGA) have suggested four-step and five-step mechanisms for the complete decomposition of composites of carbon-fibre with epoxy resin [6], [7], where complete reaction requires temperatures over 800°C. Here only data up to a temperature of approximately 280°C on the backside of the sample are considered as this is the range for which reliable expansion was measurable. TGA data from these previous studies suggests that the first reaction,

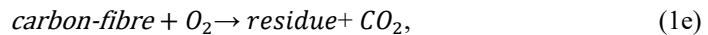


begins around 250°C and can occur without oxygen. This reaction is assumed independent of the environment – it proceeds independently if oxygen is or is not present. When oxygen is present, the second reaction occurs shortly after or nearly simultaneously for some heating rates, and is given by:



where the potential for a different char species to be created is allowed.

At hotter temperatures, the previously developed mechanism includes the additional reactions



which allow the samples to decompose almost completely to ash residue.

Because the threshold temperature for eqns (1a) and (1b) is only just achieved in the experiments reported here, this mechanism suggests that most of expansion measured up to 280°C is purely thermal expansion leading through the glass transition temperature of the epoxy. Only the initial onset of decomposition is reached, as confirmed by simulations.

### 3 EXPERIMENTS

The experimental setup is shown in Figs 2 and 3. Independent lasers were used for digital image correlation (DIC) and thermographic phosphor measurements. Additionally, visible light cameras were used to measure the thickness change in time on the edge of the sample and record video of the experiment. An IR camera was used to measure the temperature on the top of the sample. Thermocouples measured the heater and sample (backside) temperatures.

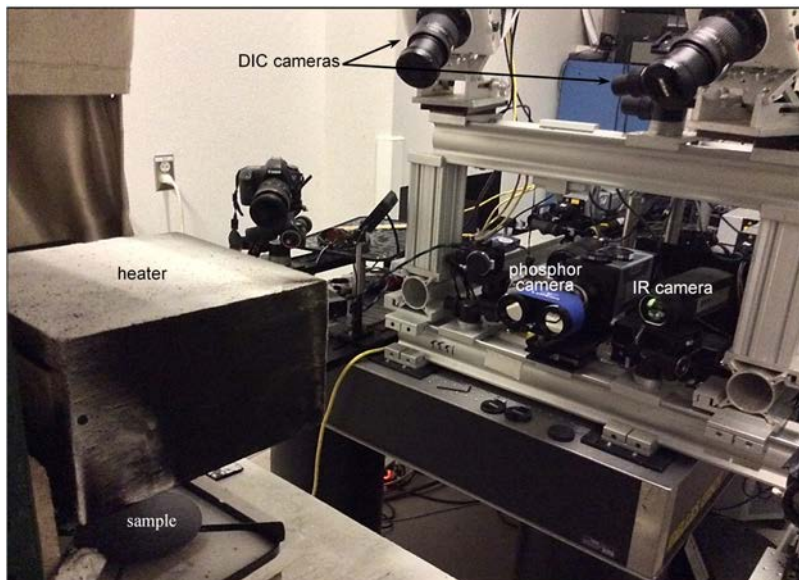


Figure 2: View with the sample in the foreground, looking back at the camera array.

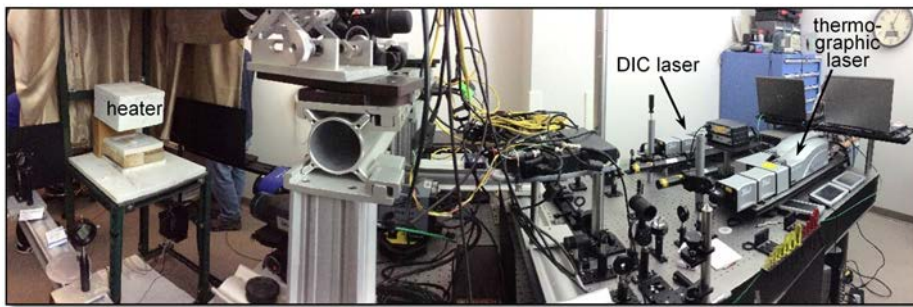


Figure 3: Panoramic view of the burn setup including lasers (far right) for DIC and thermographic phosphor measurements, camera array (centre, where the IR and visible camera are obscured), and heater and sample stage (far left).

#### 4 COMPUTATIONAL MODELING

A disk of diameter 12.7 cm and thickness 2.5 mm was meshed with three refinements of hexahedral elements, the coarsest and finest of which are shown in Fig. 4. The coarsest, intermediate and finest meshes had 2, 3 and 4 elements through the thickness, respectively. These correspond to elements with edge lengths of approximately 1.25, 0.83 and 0.625 mm, respectively. A heat flux was applied to the top surface and the bottom surface was insulated. The thermal and porous media flow was solved using the finite element code Aria, part of the Sierra suite [8].

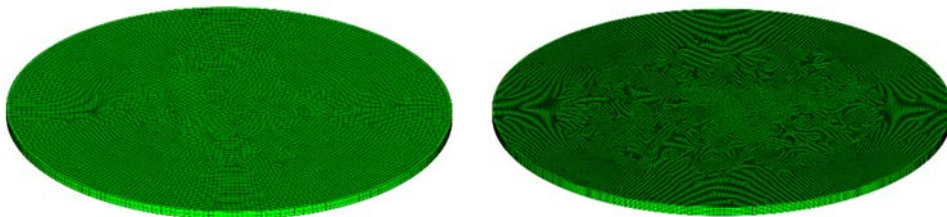


Figure 4: Images of the coarsest and finest hex meshes used for computational simulations.

The multilayer carbon-fibre composite was treated as homogeneous material until the decomposition governed by eqn (1) began. The material properties used are given in Table 1. The emissivity on the top surface was taken to be 0.91, consistent with previous studies [6].

The reaction rate  $k$  for eqn (1) is assumed to have an Arrhenius rate dependence, given by:

$$k = Ae^{-E_a/k_B T}, \quad (2)$$

where  $A$  is the pre-exponential factor,  $E_a$  is the activation energy,  $k_B$  is Boltzmann's constant, and  $T$  is the temperature in absolute units. For the only reaction initiated, eqn (1a),  $A = 3.33 \times 10^{11} \text{ s}^{-1}$  and  $E_a = 1.47 \times 10^8 \text{ J/kmol}$ . The stoichiometric coefficient of the solid phase  $char_A$  product on a mass basis is 0.5, and the heat of reaction is taken to be zero based on past differential scanning calorimetry (DSC) studies [6].

Table 1: Thermal parameters for the carbon-fibre epoxy sample from Scott et al. [6], with the exception of the temperature dependent density of epoxy.

Property	Units	Material		
		Epoxy resin	Carbon-fibre	Char
Thermal conductivity	W/m-K	0.145	$0.335 \ln(T) - 1.8257$	0.029
Density	kg/m <sup>3</sup>	$1300 + aT$	1779	650
Specific heat	J/kg-K	866	$4.0997T - 369.12$	936
Permeability	m <sup>2</sup>	$2.42 \times 10^{-15}$	$2.42 \times 10^{-14}$	$2.83 \times 10^{-12}$

#### 4.1 Mesh dependency

Three mesh resolutions with 2, 3 and 4 elements through the thickness were investigated. These had corresponding element counts of 14,440, 43,249 and 141,944. Because the heat flux applied in the experiments was relatively low, the transients were very slow. Thus it was found that this relatively course resolution was sufficient to provide nearly mesh-independent results. Over the 1700 s of interest, the temperature simulated at the bottom-centre of the sample with the finest resolution mesh was within 3.2% and 3.5% of the values from the intermediate and coarse meshes, respectively, for all time steps.

## 5 RESULTS

Initial experimental and computational results are shown here indicating that significant thermal expansion occurs as the carbon-fibre epoxy moves through its glass transition temperature. This continues with the onset of thermal decomposition. Qualitative observations not discussed here show that expansion increases more dramatically as more gas products are generated, causing the fibre layers to separate.

#### 5.1 Experimental results

A compiled set of data is shown in Fig. 5 near the end time of the experimental data of interest, at 25 min and 23 s. In Fig. 5(a) the thermocouple temperatures at the heater and below the sample are shown. Fig. 5(b) shows the IR camera image at this same time. Note that this image assumes a single emissivity, and thus is most accurate on the top surface and requires other rescaling on other surfaces, particularly the disk edge which appears unrealistically hot. It also shows the DIC markers as rows of hot spots near the centre of the disk. Finally, Fig. 5(c) shows a visible snapshot taken simultaneously to a laser firing for the internal phosphors. The DIC dots show up as a thick white band from front to back due to their excitement and overexposure by the visible light camera.

Detailed thermocouple data is shown in Fig. 6 with the corresponding heater power shown as a percentage of the maximum possible power. Based on the backside temperature, it is expected that the expansion measured in the first 1200 s should be due purely to thermal expansion. In later times, TGA data suggests that decomposition of the epoxy adhering to the mechanism in eqn (1) should begin between 1400 and 1600 s. The heater power was specifically increased in steps to move into this regime.



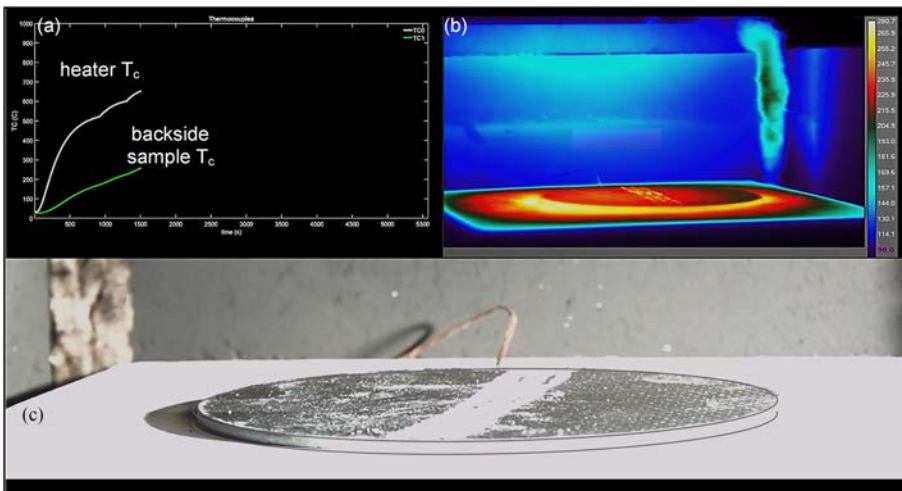


Figure 5: (a) Thermocouple temperatures at the heater and backside of sample; (b) Infrared image of the sample; and (c) Visible image at an instant illuminated by a laser.

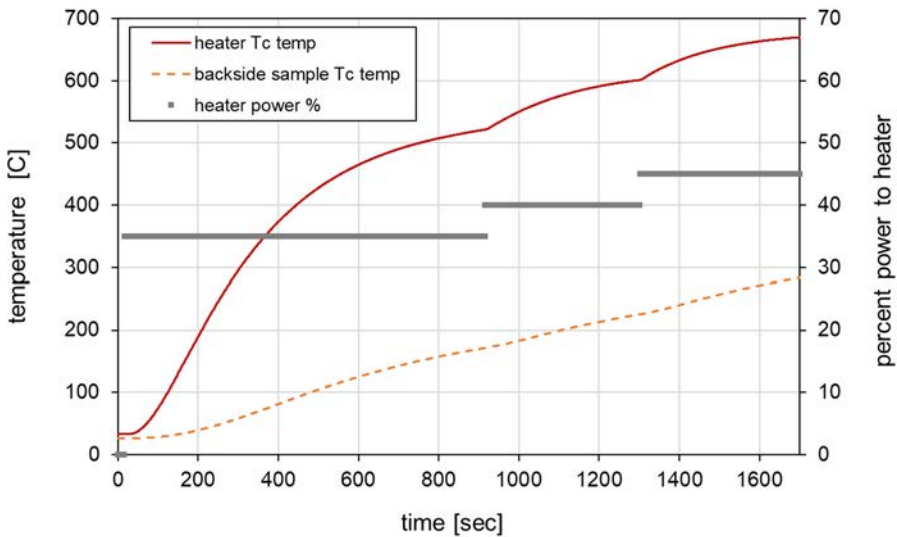


Figure 6: Temperatures (left axis) of the heater and sample backside and percent power to the heater (right axis).

Fig. 7 shows the increase of thickness near the front edge of the sample versus time. This measurement was performed by fitting a smooth surface to the entire DIC measurement field, and extrapolating that to the visible front edge measurement. There is no obvious increase in the thickness change associated with the onset of the epoxy decomposition, after the initial thermal expansion. Nevertheless, in increasing the temperature to just under 300°C on the backside, a 10% increase in sample thickness is observed.

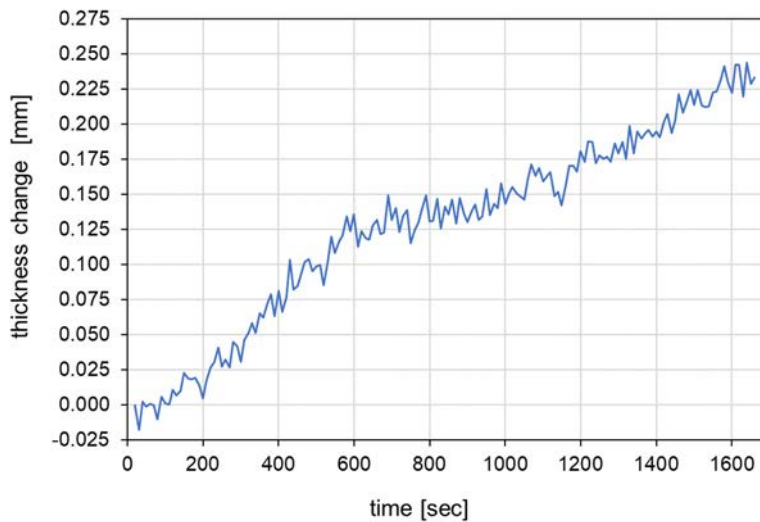


Figure 7: Average thickness change by combining visible edge measurements and a smooth fit to the DIC measurements, extrapolated to the front edge.

## 5.2 Modelling and simulation results

Model results shown in Fig. 8 demonstrate a similar temperature rise to experiments, though quantitatively the values diverge at later times. Previous research showed strongest sensitivities to the thermal properties including density, specific heat and conductivity of the bulk and/or carbon fibre, with generally less sensitivity to the permeability of the porous media flow [6].

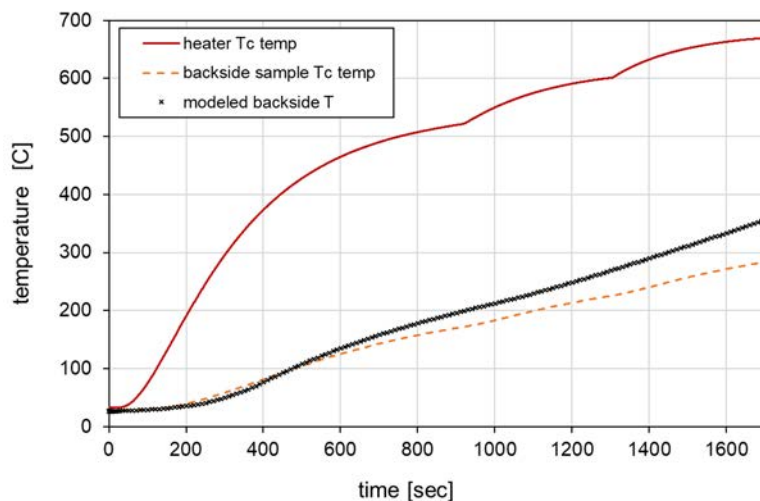


Figure 8: Modelled increase in temperature versus time at the bottom, centre of the sample, compared to the experimentally measured temperature.

Fig. 9 shows the mass fractions of the various constituents in the composite and further confirm that reactions are not expected until the very end of this experiment and model. As the epoxy begins to break down, char and fuel, the latter modelled as methane ( $\text{CH}_4$ ), begin to form as in eqn (1a). Given the overshoot of temperature of the model in Fig. 8, it is likely that even these early reactions have not initiated in the lower temperature experiment. Thus all expansion measured in Fig. 7 is likely due almost purely to thermal expansion.

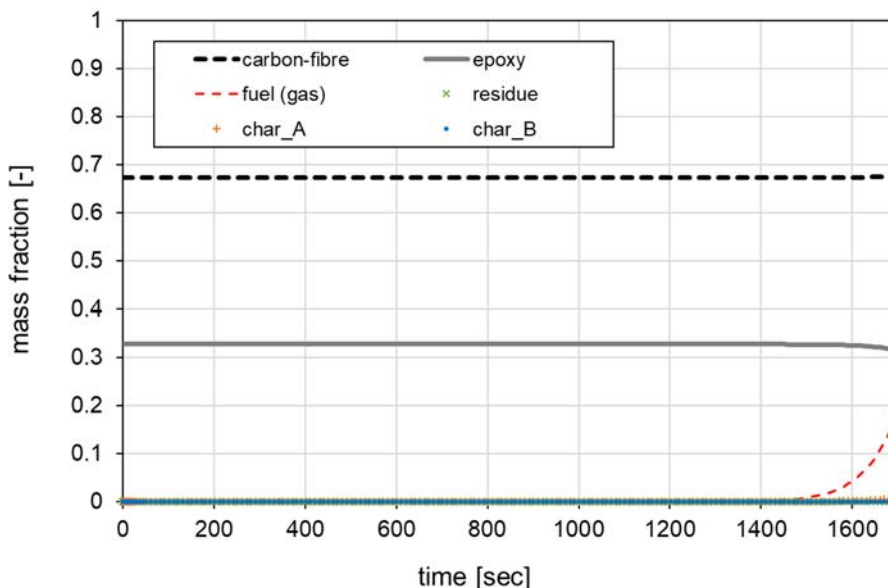


Figure 9: Simulated mass fractions of carbon-fibre, epoxy and the products of the reaction mechanisms given in eqn (1) on the backside of the sample.

By using Figs 6 and 7 in conjunction, it is possible to fit a value of the thermal expansion coefficient  $\alpha$ . However, based on recent experiments at different heating rates, this has proven to not be universal. Interestingly, for experiments with very slow heating rates, it has recently been observed that it is possible to initiate decomposition that completely offsets the thermal expansion, leading to a monotonic decrease in the thickness of the sample, rather than an increase. Thus, it appears that the coefficient of thermal expansion is dependent on not only the absolute temperature of the carbon fibre sample, but also on the temporal gradient of the heating.

### 5.3 Simulations beyond experimental results

For completeness, the extended simulation results beyond the range for which reliable experimental data is available are shown in Fig. 10 for the backside of the sample. After 1700 s the epoxy degrades quickly into flammable, gaseous fuel and  $\text{char}_A$ . At the temperatures in these simulations, the production of  $\text{char}_B$  and residue remains negligible. Around 2500 s the epoxy is depleted and production of fuel ceases. Furthermore, the temperatures needed to initiate the decompositions of  $\text{char}_A$  to residue and carbon-fibre to residue are not attained. This is consistent with the lack of ignition observed experimentally.

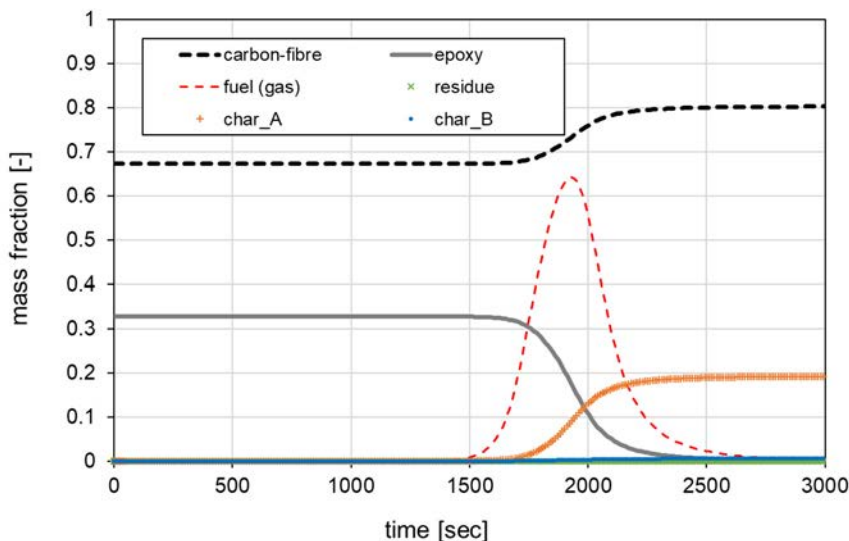


Figure 10: Simulated mass fractions of carbon-fibre, epoxy and the products of the reaction mechanisms given in eqn (1), for times beyond those in the experiment.

## 6 CONCLUSIONS

Swelling of up to 10% can be expected from heated composite flat panels, mostly due to thermal expansion even before decomposition mechanisms begin. Once decomposition begins, this effect is generally observed to be further magnified between the composite layers, eventually allowing gases to escape between the fibre layers at a much faster rate than the porous media flow through the layers in the normal direction. However, even this general finding is not universally observed as sufficiently slow heating rates appear to allow the porous media flow to offset the thermal expansion. This suggests that the decomposition reaction may occur at lower temperatures than originally believed, but further investigation is required before any definitive statement can be made.

The goal of future experiments and modelling is to quantify expansion (or contraction) and anisotropy in permeability for all the pyrolysis reaction mechanisms. Ongoing modelling efforts suggest that better agreement can be achieved by ramping the heater at a slow constant rate of power increase, and then holding the power constant for sufficient time to characterize the various decomposition mechanisms that occur, and then again ramping at constant rate. This may allow better association of each mechanism with TGA and DSC findings. Additionally, the effect of number of layers of composite is of interest. Experiments to investigate both effects are planned.

## ACKNOWLEDGEMENTS

The authors would like to acknowledge the contributions of Brian McKay for laying up the composite samples and Vince Valdez for constructing and characterizing the heater.

Sandia National Laboratories is a multi-mission laboratory managed and operated by National Technology and Engineering Solutions of Sandia, LLC, a wholly owned subsidiary of Honeywell International Inc., for the U.S. Department of Energy's National Nuclear Security Administration under contract DE-NA0003525.



#### REFERENCES

- [1] Teresko, J., Boeing 787: A matter of materials – Special report: Anatomy of a supply chain. *Industry Week*, 15 Nov. 2007.
- [2] National Transportation Safety Board, Auxiliary power unit battery fire, Japan Airlines Boeing 787-8, JA829J, Washington, DC, 2014.
- [3] McKinnon, M.B., Ding, Y., Stoliarov, S.I., Crowley, S. & Lyon, R.E., Pyrolysis model for a carbon fiber/epoxy structural aerospace composite. *J. Fire Sci.*, **35**(1), pp. 36–61, 2017.
- [4] Brubach, J., Pflitsch, C., Dreizler, A. & Atakan, B., On surface temperature measurements with thermographic phosphors: A review. *Prog. Energy Combustion Sci.*, **39**, 2013.
- [5] Flores-Brito, W., Westphal, E., Wilburn, B.R. & Hoffmeister, K.N.G., Study of sensitivity vs. excitation time of LED excited thermographic phosphor. *Proc. of the AIAA Science and Tech. Forum*, 2019.
- [6] Scott, S.N. et al., Validation and uncertainty estimation of carbon fiber epoxy composite model. *Proceedings of the 11th US National Combustion Meeting*, 2019.
- [7] Scott, S.N. et al., Modeling the decomposition behaviour of carbon fiber epoxy composite. *Proceedings of the 11th Mediterranean Combustion Symposium*, 2019.
- [8] Notz, P.K., Subia, S.R., Hopkins, M.M., Moffat, H.K., Noble, D.R. & Okusanya, T.O., *SIERRA Multimechanics Module: Aria User Manual*, 2016.

